arXiv:0704.0093v1 [cond-mat.supr-con] 1 Apr 2007

Aspects of Electron-Phonon Self-Energy Revealed from Angle-Resolved Photoemission Spectroscopy

W.S. Lee,[1] S. Johnston,[2] T.P. Devereaux,[2] and Z.-X. Shen[1]

[1]*Department of Physics, Applied Physics, and Stanford Synchrotron Radiation Laboratory, Stanford University, Stanford, CA 94305*

[2]*Department of Physics, University of Waterloo,Waterloo, Ontario, Canada N2L 3G1*

(Dated: February 8, 2022)

Lattice contribution to the electronic self-energy in complex correlated oxides is a fascinating subject that has lately stimulated lively discussions. Expectations of electron-phonon self-energy effects for simpler materials, such as Pd and Al, have resulted in several misconceptions in strongly correlated oxides. Here we analyze a number of arguments claiming that phonons cannot be the origin of certain self-energy effects seen in high-T_c cuprate superconductors via angle resolved photoemission experiments (ARPES), including the temperature dependence, doping dependence of the renormalization effects, the inter-band scattering in the bilayer systems, and impurity substitution. We show that in light of experimental evidences and detailed simulations, these arguments are not well founded.

PACS numbers: Valid PACS appear here

I. INTRODUCTION

The microscopic pairing mechanism of the high-T_c superconductivity remains an unsolved question even after twenty years of its discovery. Observations of a kink at around 40-70 meV in the band dispersion along the diagonal of the Brillouin zone (nodal diection) and a peak-dip-hump (PDH) structure at the zone boundary by angle-resolved photoemission spectroscopy (ARPES)[1,2,3,4,5,6,7,8,9,10,11,12,13] have drawn a great deal of recent attention as they may shed some light on this problem. Although an agreement has been established that the kink and PDH structure are signatures of the electrons coupled to a sharp bosonic mode, it is still strongly debated about the origin of this bosonic mode. Influenced by the fact that the high-T_c cuprate is a doped antiferromagnetic insulator, a common belief is that this bosonic mode has a magnetic origin[2,3,4,5,6,7,8,9]. However, an alternative view is that the electron-phonon coupling in such a doped-insulator can be very strong and anomalous because of a number of unusual effects, such as poor screening, complex structure as well as the interplay with correlations. Indeed, oxygen related optical phonons have been invoked to explain the temperature and doping dependence of the renormalization effects[10,11,12,13,14]. This idea of phonons being mainly responsible for this low energy band renormalization effect observed by ARPES has stimulated intense debate. There is currently no consensus whether a phonon, a set of phonons, or a magnetic mode is the primary cause of the band renormalization.

As mentioned, some important reasons to invoke phonon interpretation of the ARPES data are: the presence of an universal energy scale in all materials at all doping[10,15], particularly in the normal state of very low T_c materials[16]; the strong inferred momentum dependence[11,14]; the existence of multiple bosonic mode couplings[12] and the decrease in the overall coupling strength with increased doping, interpreted as a screening effect, especially for phonons with eigenvectors along the c-axis[13]. Yet, there is still a widespread belief that phonons are not responsible for the kink features. In the following sections, with a comprehensive look at all experimental data as well as some recent simulations, we address some of the criticisms that have been commonly used to argue against the phonon interpretation. These include the temperature and doping dependence of the renormalization effects, inter-band scattering for bilayer system, and the ARPES experiments on impurity substituted Bi2212 crystal, $Bi_2Sr_2Ca(Cu_{2-x}M_x)O_{8+\delta}$ with M = Zn or Ni. Our goal is to clarify these misconceptions as being due to oversimplifying the effects of electron-phonon coupling in cuprates as well as other strongly correlated transition metal oxides.

II. ASPECTS OF THE ELECTRON-PHONON SELF-ENERGY

A. Temperature Dependence

In the standard treatment of electron-phonon coupling effects, the Debye temperature sets a characteristic temperature scale, which is well above T_c in conventional superconducting materials. However in the cuprates and other low Fermi energy systems, these two energy scales can be comparable. As a result, the temperature dependence of phonon induced self-energies can be very different from that of conventional superconductors. According to the ARPES measurements on Bi2212 system, the band renormalization in the antinodal region (peak-dip-hump structure) shows a dramatic superconductivity-induced enhancement when the system goes through a phase transition from the normal state to the superconducting state. It has been argued that only a mode which emerges in the superconducting state and vanishes in

the normal state can explain this temperature-dependent renormalization effect[2,3,4,5]. Phonons are thereby excluded.

The sharpness of the renormalization effects due to electron-phonon coupling is strongly temperature dependent, given by the fact that T_c of optimally-doped Bi2212 is close to 100K. To demonstrate this temperature dependence, we consider the normal state (120 K) and superconducting state (10 K) of a d-wave superconductor coupled to a 36 meV B_{1g}, 55meV oxygen A_{1g}, and 70 meV breathing phonons[14,17]. The electron-phonon coupling for the B_{1g} and breathing phonons are those used in Ref. 14. The A_{1g} modes involve c-axis motions of both planar and apical oxygens, and have two branches around 55 and 80 meV. The apical electron-phonon coupling, derived in Ref. 17, involves a charge-transfer from the apex oxygen into the CuO_2 plane via the Cu 4s orbital, the same pathway that gives rise to bi-layer splitting. However, for simplicity, the apical electron-phonon coupling is treated as a constant in the calculations presented in this paper. The reason to include three modes in the calculation was inspired by the earlier success of the two-mode calculation[11] as well as the recent discovery of multiple mode coupling[12,13]. For this calculation, the tight-binding band structure described in Ref. 19 has been used. The real part and imaginary part of the self-energy $\Sigma(\mathbf{k},\omega)$ and the spectral functions $A(\mathbf{k},\omega)$ at $k=(0,\pi)$ are then obtained within weak coupling Eliashberg formalism[14] and plotted in Fig. 1. Details of the calculations are presented in the Appendix.

At high temperature, both $\mathrm{Re}\Sigma(\mathbf{k},\omega)$ and $\mathrm{Im}\Sigma(\mathbf{k},\omega)$ do not exhibit a sharp renormalization feature as shown by the dashed curves in Fig. 1 (a) and Fig. 1(b), respectively. This demonstrates that the thermal broadening effect smears out the sharp renormalization features; in addition, broadening effects due to additional many body effects would smear out the renormalization features further. Thus, one should not expect to observe any sharp renormalization features at $k=(0,\pi)$ in the normal state ($\sim$ 100K) from the electron-phonon coupling. In the superconducting state, the renormalization features of the self-energy become much sharper, due to smaller thermal broadening effect as well as the opening of a superconducting gap. Consistent with the optimally-doped Bi2212 and Bi2223 measurements[2,4,11,18], the PDH structure of the spectral function at $k=(0,\pi)$ emerges at low temperature and disappears at high temperature (normal state), as illustrated in Fig. 1(c) and Fig. 1(d), respectively. While this behavior is generally expected for any phonon, we note that in addition, the self-energy from electron-phonon couplings which involve momentum transfers within and between anti-nodal regions of the Fermi surface, such as the apex A_{1g} and B_{1g} phonons, are greatly enhanced for all k-points due to the large density of state enhancements in these regions via the opening of a d-wave gap. A detailed momentum dependence of the renormalization effects in the normal state and superconducting state due to the coupling to the B_{1g} phonon has been discussed in Ref. 11 and Ref. 14. Furthermore, both the dispersion kink and the PDH structure in the nodal region have been clearly observed in the normal state when measured at a low temperature on samples with a lower T_c[16]. This lends further support to the strongly temperature dependent renormalization features due to electron-phonon coupling.

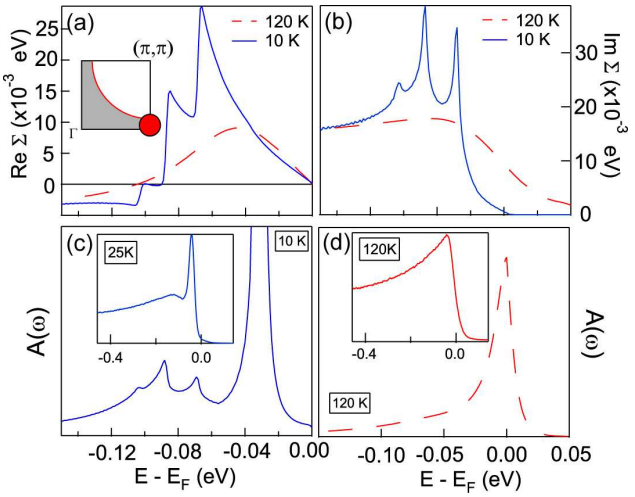


FIG. 1: The calculated (a) real part, ReΣ, (b) imaginary part of the self-energy, ImΣ , and the corresponding spectral functions, A(k,ω) in (c) normal state and (d) superconducting state. An extra 5 meV is added to the imaginary part of the self energy in 120K simulation to account for the thermal broadening of the quasi-particle life time. The location for this calculation is indicated in inset of (a) by a red dot with a red curve representing the FS. Insets of (c) and (d) are the data of optimally-doped Bi2223 system (T_c=110K) taken at the normal state (120K) and superconducting state(25K)[18], respectively.

B. Doping Dependence

Another problematic statement against the phonon scenario stems from the apparent strong doping dependence of the kink position and strength. Based on the wisdom for conventional good metals, phonons should not have a strong doping dependence, either in frequency of the mode or in strength of the coupling. This is not necessary valid for layered, doped insulators with strong correlation effects, such as cuprates where doping dramatically changes the metallicity and the ability of electrons to screen charge fluctuations. We first note that many experiments on various cuprates have reported strongly doping dependent anomalies for several phonons, which implies a strongly doping dependent e-p coupling for these phonons. For example, from inelastic neutron scattering measurements, the breathing mode, half-breathing mode, and the bond-stretching modes exhibit prominent doping dependence of dispersion and energy renormalizations[20,21]. In Raman and infrared spec-

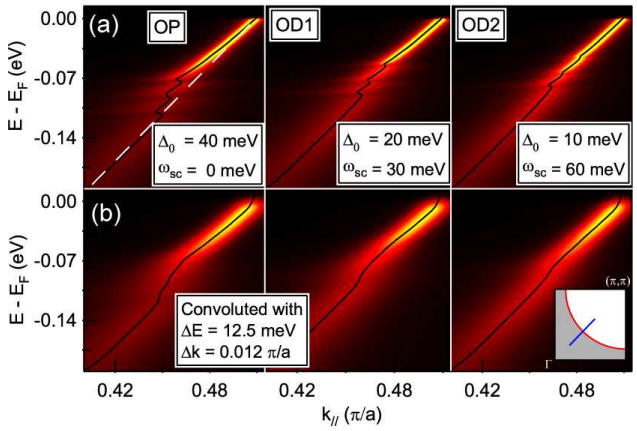


FIG. 2: The intensity plots of the (a) spectral functions without resolution convolution and (b) resolution convoluted spectral functions in the superconducting state (10K) along the nodal direction, as indicated in the inset of (b) by the blue line. Black curves are the band dispersion extracted from the maximum positions of the momentum distribution curves, which cut the spectral functions at a fixed energy. The MDC-derived dispersions in (a) exhibit three sharp "subkinks" due to the coupling to the three phonon modes used in the model; while in (b) the subkinks are washed out by the finite instrument resolution effect leaving an apparent single kink in the band dispersion. The white dashed line illustrates the bare band for extracting ReΣ shown in Fig. 3 (a).

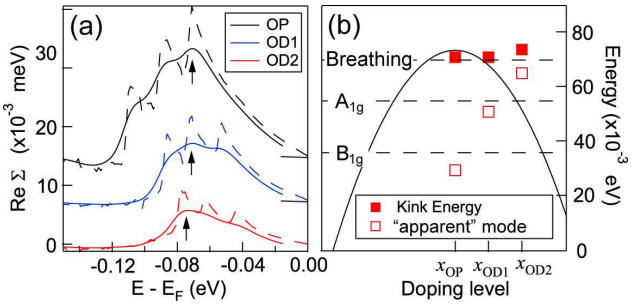


FIG. 3: (a) The ReΣ extracted from Fig. 2(a) (dashed lines) and Fig. 2(b) (solid lines) by subtracting a linear bare band (dashed line in Fig. 2(a)) from the band dispersion. The arrows indicate the maximum positions of the ReΣ where the "single" apparent kink in the band dispersion is usually defined. (b) Summary of the doping dependence of the apparent kink energy and the apparent mode energy extracted by assuming a single mode scenario.

troscopy, the Fano lineshapes of phonon modes in B_{1g} and B_{1u} symmetry show strong doping dependences[22]. Furthermore, the strength of the phonon energy shift and linewidth variation across T_c also changes strongly with doping[23].

Second, the doping dependence of the renormalization effects to the electronic self-energy is sophisticated as inferred by two recent ARPES studies. One is the observation of multiple bosonic mode couplings along the nodal direction[12]. The other is the doping dependence of the c-axis screening effect to the coupling between the electron and $c-$axis phonons. As proposed by Meevasana *et al.*[13,24] and Devereaux *et al.*[17], for electron-phonon coupling at long wavelengths, the screening becomes more effective at reducing the coupling strength when the c-axis conductivity becomes more metallic. Given these two results plus the variation of the superconducting gap magnitude with doping, the doping dependence of the kink energy is highly convoluted in Bi2212 whose superconducting gap has an energy comparable to some of the phonons.

In Fig. 2, we present the intensity plot of calculated spectral functions demonstrating a doping dependence of the dispersion kink in the superconducting state. The superconducting gap size was set to be 40, 20, and 10 meV for the optimally-doped and more overdoped systems. In addition, the coupling strength of the breathing mode, whose appreciable coupling is only for short wavelengths and large momentum transfers[20,21], remains unchanged for our doping dependence simulation; while, a filter function, $\omega^2/(\omega^2+\omega_{sc}^2)$ with different value of c-axis screening frequency ω_{sc} is applied to the c-axis phonons (B_{1g} and A_{1g}), to simulate the doping-dependent coupling strength due to the change of the c-axis screening effect[13,24]. We note that although this is a simplification, it represents the general behavior of screening considerations for phonons involving small in-plane momentum transfers. Full consideration of screening has been given in Ref. 17 and Ref. 24. In addition, a component $0.005+\omega^2$ eV is added in the imaginary part of the self-energy to mimic the quasiparticle life time broadening due to electron-electron interaction.

As shown in Fig. 2(a), the coupling to multiple phonon modes induces several "subkinks" in the dispersion. The positions of these subkinks mostly correspond to the energies of phonons plus the maximum d-wave SC gap, Δ_0, even through there is no gap along the nodal direction. This is because when calculating the self-energy, one needs to integrate the contributions from the entire zone, which makes the electrons in the nodal region "feel" the presence of the gap. Furthermore, revealed by the extracted real-part of the self-energy, ReΣ (dashed curves in Fig. 3 (a)), the dominant feature in ReΣ for the OP case is induced by 36 meV B_{1g} mode, while for the OD1 and OD2 case, the features of the 55 meV A_{1g} mode and 70 meV breathing mode gradually out-weight the contribution from the B_{1g} mode. This demonstrates that the change of the SC gap magnitude and the increasing screening effect to these phonons because of increased doping alters the relative strength of the subkinks caused by different modes.

To simulate the experimental data, we convoluted the spectral functions shown in Fig. 2(a) with a typical ARPES instrumental resolution: 12.5 meV in energy resolution and 0.012 π/a in momentum resolution. As illustrated in Fig. 2(b) and the extracted ReΣ (solid curves in Fig. 3(a)), the subkinks are less obvious and become

a broadened "single" kink in the dispersion which is located at roughly the energy of the dominant phonon feature determined by the maximum position of the ReΣ (the arrows in Fig. 3(a)). The doping dependence of the kink position is summarized as the solid symbols in Fig. 3(b). Assuming a single mode scenario, one can obtain the "doping dependence" of the mode energy by subtracting out the SC gap size. However, we note that this extracted "apparent" mode energy does not match any of the modes used in the model; instead, it is a average between the dominant features (open symbols in Fig. 3(b). Clearly, since the kink energy is a sum of the superconducting gap and a spectrum of bosonic modes, it should not be taken as a precise measurement of the energy of any particular bosonic mode. This casts doubts to the analysis of the doping dependent properties of the kink in the nodal band dispersion based on the single bosonic mode coupling scenario[7,8]. More importantly, this illustrates the complex nature of lattice effects in these oxides.

C. Interband Scattering

Borisenko *et al.*[8,9] observed that the scattering rate of the bonding and antibonding bands along the nodal direction cross each other near the energy of the Van Hove singularity, suggesting a strong inter-band scattering between the bonding and antibonding bands. They argued that only a mode with "odd" symmetry, such as spin resonance mode, can mediate such inter-band scattering. The question whether phonons can induce such inter-band scattering has also been raised by these authors.

First, we note that recent high energy and momentum resolution ARPES experiments on Bi2212 using low energy photons(<10 eV) have better resolved the bilayer splitting at the nodal point[25]. However, as shown in Fig. 2 of Ref. 25, the scattering rate of the bonding and antibonding band does *not* exhibit a crossover behavior as reported by Borisenko *at al.*. The inconsistency of the data between the two groups implies that more experiments and better analysis are needed to verify whether this inter-band scattering effect is genuine.

Second, empirically, it has been known for over 15 years that interband electron-phonon coupling in the cuprates is very large. The evidence comes from the strong resonance profiles of many Raman active phonons, which display large intensity variations[26]. This is generally understood as a result of strong interband coupling, whereby phonons can be brought in and out of resonances via tuning of the incident photon energy[27]. Since, in general, phonons can also provide momentum to scatter electrons along the c-axis, direct inter bi-layer scattering can occur which involves mixing of different symmetries of phonons. This can be viewed in a simplified way even if we first neglect direct interband scattering and consider a bilayer system coupled to $c-$axis phonons. For $q_z = 0$, a simple classification of c-axis modes is possible:

$$H = \sum_{k,\sigma,\alpha=1,2} \epsilon_\alpha(k) c^\dagger_{k,\alpha,\sigma} c_{k,\alpha,\sigma} + \frac{1}{2}\sum_{k,\sigma} t_\perp(k) \left[c^\dagger_{k,1,\sigma} c_{k,2,\sigma} + h.c.\right] + \sum_{k,q,\sigma,\alpha=1,2,\nu} g_{\nu,\alpha}(k,q) \left\{c^\dagger_{k+q,\alpha,\sigma} c_{k,\alpha,\sigma} \left[a_\nu(-q) + a^\dagger_\nu(q)\right] + h.c.\right\}, \quad (1)$$

where α is the index for the electronic states of different layers, $\epsilon_1(k) = \epsilon_2(k)$, $t_\perp(k)$ describes the hopping of electrons between two layers, and the index ν can be either gerade or ungerade active c-axis modes, with symmetry classification with respect to the displacement eigenvectors to the inversion center of the cell, depicted in Fig. 4. After diagonalizing the first two terms by canonical transformation, the electron-phonon coupling can be recast as

$$H^{(g,u)}_{e-ph} = \sum_{k,q,\sigma} g_{(g,u)}(k,q) \left\{ \left[a_{(g,u)}(q) + a^\dagger_{(g,u)}(-q)\right] \times \left[c^\dagger_{k+q,+,\sigma} c_{k,(+,-),\sigma} + c^\dagger_{k+q,-,\sigma} c_{k,(-,+),\sigma}\right] + h.c.\right\} \quad (2)$$

We have used the c_+ and c_- for the even and odd linear combination of c_1 and c_2, and subscript g and u for the gerade and ungerade mode, respectively. Thus for $q_z = 0$, where this classification is possible, gerade phonons induce intra-band scattering (even channel), while the ungerade phonons mediate the interband scattering process (odd channel) even without direct electron-phonon coupling across the layers. Yet for $q_z = \pi/c$, the classification inverts, where gerade modes become ungerade and vice-versa, as illustrated in Fig 4. Thus, even in this simple case, modes at different q_z contribute both to intra and interband scattering, and the net weight of the coupling appearing in the self energy is then largely determined by the specific momentum structure $g(k,q)$. Since the self-energy generally involves sums over q_z, and coupling directly of electrons in adjacent layers via phonons are non-negligible, clearly the inter-band scattering phenomena can not be used to argue against

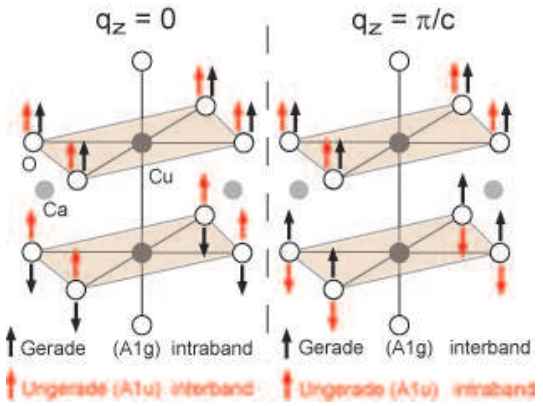


FIG. 4: The illustration of the gerade and ungerade $c-$axis phonons. The eigenmode of the gerade (ungerade) phonons is even (odd) with respect to the mirror plane between two CuO_2 layers at $q_z = 0$, while their definition swapped at $q_z = \pi/c$. The black, grey, and white circles represent the Cu, Ca, and O atoms, respectively.

the phonons being important to the electronic states.

We also add a remark concerning the electron-phonon coupling derived from Raman measurements[28] in $YBa_2Cu_3O_7$ and Bi-2212 compared to that obtained from ARPES. While one might naively expect the couplings to be comparable from Raman and ARPES, we remark that this situation is remarkably different if the coupling is strongly moment dependent and whenever correlations are appreciable. Since Raman measures phonons with net zero momentum transfer and ARPES involves a sum over all transfers, a sizeable coupling difference may be discernable. This is specifically the case for the B_{1g} phonon, where scattering involving momentum transfers across the necks of the Fermi surface near $(\pi, 0)$[14], further enhanced via correlations[29], yields a strong contribution to the electron self-energy that is absent in phonon self-energies. Moreover, a sum rule analysis presented in Ref. 30 highlights in general how electron and phonon self-energies may be qualitatively different in strongly correlated systems.

D. ARPES Experiments on Zn and Ni substituted Bi2212

In this section, we comment on recent experiments about the renormalization effects in Zn and Ni substituted Bi2212 crystal[31,32]. The strength of sharp renormalizations in these substituted crystals is found to be weakened compared to the pristine crystals. Since the magnetic properties are expectedly modified due to the Cu substitution by these impurities, the authors concluded that the sharp renormalization effects are induced by magnetic-related modes, not phonons.

In fact, a close examination of the data published by V. B. Zabolotnyy *et al.*[31] and K. Terashima *et al.*[32] implies that the magnetic property is not the only modification due to the substitution by Zn and Ni. First, although both sets of data are consistent in the antinodal region where the strength of the band renormalization is reduced, they are inconsistent with each other on the kink strength along the nodal direction. In the data set of V. B. Zabolotnyy *et al.*, the kink strength is weaker in the Zn or Ni doped samples, whereas there is no detectable change in the data set reported by K. Terashima *et al.*.

Second, the data from K. Terashima *et al.* (Fig. 1(d)-(f) in Ref. 32) suggest that the bilayer-splitting structure is much clearer in the pristine crystals than in the Zn and Ni doped crystals. Since the authors have ruled out the possibility of a significant doping level difference between pristine and impurity-doped crystals, the distinct visibility variation of the bilayer structure implies a impurity-related change in the electronic structure.

From these two observations on their data, it implies that not only the magnetic properties could change, the band structure and scattering behaviors could also be affected due to these impurities. It is possible that these changes of the electronic structures could "weaken" the renormalizaton features observed in the ARPES spectrum. Furthermore, we note that the strength of electron-phonon coupling could also be modified by the substituted impurities: this can be inferred from the change of the Fano spectra lineshape of the B_{1g} 340 cm^{-1} phonon in Raman spectral for Zn-doped YBCO[33] and Th-doped YBCO[34] resulting from an increase in the phonon linewidth due to impurity scattering. Therefore, the experiments on Ni and Zn substituted Bi2212 crystals are inconclusive experiments to distinguish phonon and magnetic modes as the origin of the renormalization effects.

III. CONCLUSION

We have shown that the temperature and doping dependence of the renormalization effects, inter-band band scattering, and the results of Zn and Ni doped materials can be understood in the framework of electron-phonon coupling. On the other hand, the issues that make it not plausible for the sharp kink being of spin origin, especially the spin resonance mode, remain: i) the nearly constant energy scale as a function of doping in small gap system[12]; ii) the multiple modes[12]; iii) the presence of clear kink in the normal state[4,13,16] iv) the detailed agreement between B_{1g} phonon based explanation of the mode coupling as a function of momentum[11,14], while the spin resonance with tiny spectral weight (2%) is unlikely to give an explanation for both nodal and antinodal renormalization; v) the accumulated evidence for lattice polaron effect in underdoped and deeply underdoped systems[35,36]. With these weaknesses of the spin resonance interpretation, lattice effect is a more plausible explanation of the renormalization effects. It remains a possibility that the spin-fluctuation and other strong correlation effects are also very important to determine the

electronic structure of cuprates; they likely contribute to a smooth renormalization of the band and may be more relevant to the higher binding energy. However, optical phonons are the most probable origin for the renormalization effects due to sharp modes near 40-70 meV, which is also supported by the recent finding of STM experiments[37,38].

Acknowledgments

W.S. Lee acknowledge the support from SSRL which is operated by the DOE Office of Basic Energy Science, Division of Chemical Science and Material Science under contract DE-AC02-76SF00515. T. P. Devereaux would like to acknowledge support from NSERC, ONR grant N00014-05-1-0127 and the A. von Humboldt Foundation.

APPENDIX A: MIGDAL-ELIASHBERG BASED APPROACH

In the calculations presented herein, we evaluate electronic self energies and spectral functions via Migdal-Eliashberg treatment, as discussed in Ref. 39. The dressed Green's function in the superconducting state is given in Nambu notation by

$$\hat{G}(\mathbf{k},\omega) = \frac{\omega Z(\mathbf{k},\omega)\hat{\tau}_0 + [\epsilon(\mathbf{k}) + \chi(\mathbf{k},\omega)]\hat{\tau}_3 + \phi(\mathbf{k},\omega)\hat{\tau}_1}{[\omega Z(\mathbf{k},\omega)]^2 - [\epsilon(\mathbf{k}) + \chi(\mathbf{k},\omega)]^2 - \phi^2(\mathbf{k},\omega)}, \tag{A1}$$

from which the spectral function follows $A(\mathbf{k},\omega) = -\frac{1}{\pi}G''_{1,1}(\mathbf{k},\omega)$ as shown in Figs. 1c,1d, and 2. The momentum-dependent components of the Nambu self energy are given as generalizations of those found in Ref. 39:

$$\omega Z_2(\mathbf{k},\omega) = \frac{\pi}{2N}\sum_{\mathbf{p},\nu} |g_\nu(\mathbf{k},\mathbf{p}-\mathbf{k})|^2 \big([n_b(\Omega_\nu) + n_f(E_\mathbf{p})][\delta(\omega+\Omega_\nu - E_\mathbf{p}) + \delta(\omega-\Omega_\nu+E_\mathbf{p})] \\ + [n_b(\Omega_\nu) + n_f(-E_\mathbf{p})][\delta(\omega-\Omega_\nu-E_\mathbf{p}) + \delta(\omega+\Omega_\nu+E_\mathbf{p})]\big) \tag{A2}$$

$$\chi_2(\mathbf{k},\omega) = -\frac{\pi}{2N}\sum_{\mathbf{p},\nu} |g_\nu(\mathbf{k},\mathbf{p}-\mathbf{k})|^2 \frac{\epsilon_\mathbf{p}}{E_\mathbf{p}}\big([n_b(\Omega_\nu) + n_f(E_\mathbf{p})][\delta(\omega+\Omega_\nu - E_\mathbf{p}) - \delta(\omega-\Omega_\nu+E_\mathbf{p})] \\ + [n_b(\Omega_\nu) + n_f(-E_\mathbf{p})][\delta(\omega-\Omega_\nu-E_\mathbf{p}) - \delta(\omega+\Omega_\nu+E_\mathbf{p})]\big) \tag{A3}$$

$$\phi_2(\mathbf{k},\omega) = \frac{\pi}{2N}\sum_{\mathbf{p},\nu} |g_\nu(\mathbf{k},\mathbf{p}-\mathbf{k})|^2 \frac{\Delta_\mathbf{p}}{E_\mathbf{p}}\big([n_b(\Omega_\nu) + n_f(E_\mathbf{p})][\delta(\omega+\Omega_\nu - E_\mathbf{p}) - \delta(\omega-\Omega_\nu+E_\mathbf{p})] \\ + [n_b(\Omega_\nu) + n_f(-E_\mathbf{p})][\delta(\omega-\Omega_\nu-E_\mathbf{p}) - \delta(\omega+\Omega_\nu+E_\mathbf{p})]\big) \tag{A4}$$

where ν denotes the phonon mode index, and n_f and n_b are the Fermi and Bose occupation factors. $g_\nu(\mathbf{k},\mathbf{q})$ are the corresponding electron-phonon couplings for mode ν, given in reference[14] for the B_{1g} and breathing modes. We choose to model the A_{1g} coupling via a momentum independent coupling. Further details can be found in Ref. 17.

[1] P. V. Bogdanov, A. Lanzara, S. A. Kellar, X. J. Zhou, E. D. Lu, W. J. Zheng, G. Gu, J.-I. Shimoyama, K. Kishio, H. Ikeda, R. Yoshizaki, Z. Hussain, and Z. X. Shen, Phys. Rev. Lett. **85**, 2581 (2000).

[2] A. Kaminski, M. Randeria, J. C. Campuzano, M. R. Norman, H. Fretwell, J. Mesot, T. Sato, T. Takahashi, and K. Kadowaki, Phys. Rev. Lett. **86**, 1070 (2001).

[3] T. K. Kim, A. A. Kordyuk, S. V. Borisenko, A. Koitzsch, M. Knupfer, H. Berger, and J. Fink, Phys. Rev. Lett. **91**, 167002 (2003).

[4] T. Sato, H. Matsui, T. Takahashi, H. Ding, H.-B. Yang, S.-C. Wang, T. Fujii, T. Watanabe, A. Matsuda, T. Terashima, and K. Kadowaki, Phys. Rev. Lett. **91**, 157003 (2003).

[5] M. R. Norman, H. Ding, J. C. Campuzano, T. Takeuchi, M. Randeria, T. Yokoya, T. Takahashi, T. Mochiku, and K. Kadowaki, Phys. Rev. Lett. **79**, 3506 (1997).

[6] A. D. Gromko, A. V. Fedorov, Y.-D. Chuang, J. D. Koralek, Y. Aiura, Y. Yamaguchi, K. Oka, Yoichi Ando, and D. S. Dessau Phys. Rev. B **68**, 174520 (2003)

[7] A. A. Kordyuk, S. V. Borisenko, V. B. Zabolotnyy, J. Geck, M. Knupfer, J. Fink, B. Büchner, C. T. Lin, B. Keimer, H. Berger, A.V. Pan, Seiki Komiya, and Yoichi Ando, Phys. Rev. Lett. **97**, 017002(2006).

[8] S. V. Borisenko, A. A. Kordyuk, V. Zabolotnyy, J. Geck, D. Inosov, A. Koitzsch, J. Fink, M. Knupfer, B. Büchner, V. Hinkov, C. T. Lin, B. Keimer, T. Wolf, S. G. Chiuzbăian, L. Patthey, and R. Follath, Phys. Rev. Lett. **96**, 117004 (2006).

[9] S. V. Borisenko, A. A. Kordyuk, A. Koitzsch, J. Fink, J. Geck, V. Zabolotnyy, M. Knupfer, B. Büchner, H. Berger, M. Falub, M. Shi, J. Krempasky, and L. Patthey, Phys. Rev. Lett. **96**, 067001 (2006).

[10] A. Lanzara, P. V. Bogdanov, X. J. Zhou, S. A. Kellar, D. L. Feng, E. D. Lu, T. Yoshida, H. Eisaki, A. Fujimori, K. Kishio, J.-I. Shimoyama, T. Noda, S. Uchida, Z. Hussain, Z.-X. Shen, Nature (London) **412**, 510 (2001).

[11] T. Cuk, F. Baumberger, D. H. Lu, N. Ingle, X. J. Zhou, H. Eisaki, N. Kaneko, Z. Hussain, T. P. Devereaux, N. Nagaosa, and Z.-X. Shen, Phys. Rev. Lett. **93**, 117003 (2004).

[12] X. J. Zhou, Junren Shi, T. Yoshida, T. Cuk, W. L. Yang, V. Brouet, J. Nakamura, N. Mannella, Seiki Komiya, Yoichi Ando, F. Zhou, W. X. Ti, J. W. Xiong, Z. X. Zhao, T. Sasagawa, T. Kakeshita, H. Eisaki, S. Uchida, A. Fujimori, Zhenyu Zhang, E. W. Plummer, R. B. Laughlin, Z. Hussain, and Z.-X. Shen, Phys. Rev. Lett. **95**, 117001 (2005).

[13] W. Meevasana, N. J. C. Ingle, D. H. Lu, J. R. Shi, F. Baumberger, K. M. Shen, W. S. Lee, T. Cuk, H. Eisaki, T. P. Devereaux, N. Nagaosa, J. Zaanen, and Z.-X. Shen, Phys. Rev. Lett. **96**, 157003 (2006).

[14] T. P. Devereaux, T. Cuk, Z.-X. Shen, and N. Nagaosa, Phys. Rev. Lett. **93**, 117004 (2004).

[15] X.J. Zhou, T. Yoshida, A. Lanzara, P.V. Bogdanov, S.A. Kellar, K.M. Shen, W.L. Yang, F. Ronning, T. Sasagawa, T. Kakeshita, T. Noda, H. Eisaki, S. Uchida, C.T. Lin, F. Zhou, J.W. Xiong, W.X. Ti, Z.X. Zhao, A. Fujimori, Z. Hussain, and Z.-X. Shen, Nature **423**, 398 (2003).

[16] A. Lanzara, P. V. Bogdanov, X. J. Zhou, N. Kaneko, H. Eisaki, M. Greven, Z. Hussain, and Z. -X. Shen, cond-mat/0412178.

[17] T. P. Devereaux, Z.-X. Shen, N. Nagaosa, and J. Zaanen, preprint.

[18] W.S. Lee *et al.*, unpublished.

[19] M. Eschrig and M. R. Norman, Phys. Rev. B **67**, 144503 (2003).

[20] L. Pintschovius, Phys. stat. sol. (b) **242**, 30 (2005), and the references herein.

[21] D. Reznik, L. Pintschovius, M. Ito, S. Likubo, M. Sato, H. Goka, M. Fujita, K. Yamada, G. D. Gu, and J. M. Tranquada, Nature **440**, 1170 (2006).

[22] M. Opel, R. Hackl, T. P. Devereaux, A. Virosztek and A. Zawadowski, A. Erb and E. Walker, H. Berger and L. Forró, Phys. Rev. B **60**, 9836 (1999); C. Bernhard, D. Munzar, A. Golnik, C. T. Lin, A. Wittlin, J. Humlíček, and M. Cardona, *ibid.* **61**, 618-626 (2000).

[23] E. Altendorf, X. K. Chen, J. C. Irwin, R. Liang and W. N. Hardy, Phys. Rev. B **47**, 8140(1993); K. C. Hewitt, X. K. Chen, C. Roch, J. Chrzanowski, J. C. Irwin, E. H. Altendorf, R. Liang, D. Bonn, and W. N. Hardy, *ibid.* **69** 064514(2004).

[24] W. Meevasana, T. P. Devereaux, N. Nagaosa, Z.-X. Shen, and J. Zaanen, Phys. Rev. B **74**, 174524 (2006).

[25] T. Yamasaki, K. Yamazaki, A. Ino, M. Arita, H. Namatame, M. Taniguchi, A. Fujimori, Z.-X. Shen, M. Ishikado, and S. Uchida, cond-mat/0603006.

[26] E. T. Heyen, S. N. Rashkeev, I. I. Mazin, O. K. Andersen, R. Liu, M. Cardona, and O. Jepsen, Phys. Rev. Lett. **65**, 3048-3051 (1990); B. Friedl, C. Thomsen, H.-U. Habermeier, and M. Cardona, Solid State Commun. **78**, 291 (1991); D. Reznik, S.L. Cooper, M.V. Klein, W.C. Lee, D.M. Ginsberg, A.A. Maksimov, A.V. Puchkov, I.I. Tartakovskii, and S-W. Cheong, Phys. Rev. B **48**, 7624 (1993); M. Kang, G. Blumberg, M. V. Klein, and N. N. Kolesnikov Phys. Rev. Lett. **77**, 4434 (1996); X. Zhou, M. Cardona, D. Colson, and V. Viallet, Phys. Rev. B **55**, 12 770 (1997); V.G. Hadjiev, X. Zhou, T. Strohm, M. Cardona, Q.M. Lin, and C.W. Chu, *ibid.* **58**, 1043 (1998).

[27] See, e.g., E. Ya. Sherman and C. Ambrosch-Draxl, Phys. Rev. B **62**, 9713 (2000), and references therein.

[28] Considering Y-123 and Bi-2212, earlier Raman measurements, when fit with a Fano profile, indicated that B_{1g} coupling in Y-123 is more appreciable than in Bi-2212, which was thought to be due to the different electrostatic environment surrounding the CuO_2 planes. [T.P. Devereaux, A. Virosztek, A. Zawadowski, M. Opel, P.F. Müller, C. Hoffmann, R. Philipp, R. Nemetschek, R. Hackl, H. Berger, L. Forro, A. Erb, and E. Walker, Solid State Commun. **108**, 407 (1998)]. This at the time was supported by electrostatic calculations of the c-axis oriented crystal field in Y-123 [J. Li and J. Ladik, Solid State Commun. **95**, 35 (1995)], but no calculations had been performed for Bi2212. A reexamination of the Raman data indicate that the extracted coupling for Bi-2212 may be affected by intrinsic inhomogeneity of phonon lines in Bi-2212 compared to Y-123, as well to differences in the B_{1g} electronic background. While λ was estimated to be 0.0013, with inhomogeneity of the phonon line taken into account along with a different choice of background, $\lambda = 0.02$ may be obtained, comparable to Y-123. This is supported by recent Ewald calculations for Bi-2212, which gives a value of local crystal field 1.25 eV/cm, comparable to that obtained for Y-123.

[29] Carsten Honerkamp, Henry C. Fu, and Dung-Hai Lee, cond-mat/0605161.

[30] O. Rösch, and O. Gunnarsson, Phys. Rev. Lett. **93**, 237001(2004); O. Rösch, G. Sangiovanni, and O. Gunnarsson, cond-mat/0607612.

[31] V. B. Zabolotnyy, S.V. Borisenko, A. A. Kordyuk, J. Fink, J. Geck, A. Koitzsch, M. Knupfer, B. Büchner, H. Berger, A. Erb, C. T. Lin, B. Keimer, and R. Follath, Phys. Rev. Lett. **96**, 037003 (2006).

[32] K. Terashima, H. Matsui, D. Hashimoto, T. Sato, T. Takahashi, H. Ding, T. Yamamoto AND K. Kadowaki, Nature Physics **2**, 27 (2006).

[33] M. Limonov, D. Shantsev, S. Tajima, and A. Yamanaka, Phys. Rev. B **65**, 024515(2001).

[34] E. Altendorf, J. C. Irwin, W. N. Hardy, and R. Liang, Physica C **185-189**, 1375(1991).

[35] K.M. Shen, F. Ronning, D.H. Lu, W.S. Lee, N.J.C. Ingle, W. Meevasana, F. Baumberger, A. Damascelli, N.P. Armitage, L.L. Miller, Y. Kohsaka, M. Azuma, M. Takano, H. Takagi, and Z.-X. Shen, Phys, Rev. Lett. **93**, 267002(2004)

[36] O. Rösch, O. Gunnarsson, X. J. Zhou, T. Yoshida, T. Sasagawa, A. Fujimori, Z. Hussain, Z.-X. Shen, and S. Uchida, Phys. Rev. Lett. **95**, 227002 (2005).

[37] Jinho Lee, K. Fujita, K. McElroy, J. A. Slezak, M. Wang, Y. Aiura, H. Bando, M. Ishikado, T. Masui, J.-X. Zhu, A. V. Balatsky, H. Eisaki, S. Uchida and J. C. Davis, Nature

442, 546(2006).

[38] Jian-Xin Zhu, A. V. Balatsky, T. P. Devereaux, Qimiao Si, J. Lee, K. McElroy, and J. C. Davis, Phys. Rev. B **73**, 014511(2006); cond-mat/0507621.

[39] D. J. Scalapino, in *Superconductivity, Vol. 1*, editted by R. Parks, Dekker, 1969.